Catal Lett (2009) 128:25–30
DOI 10.1007/s10562-008-9694-z

On the Characterisation of Silver Species for SCR of NO_x with Ethanol

Andrea Musi · Pascale Massiani · Dalil Brouri · Jean-Michel Trichard · Patrick Da Costa

Received: 18 July 2008 / Accepted: 22 September 2008 / Published online: 15 October 2008

Abstract Reducing of nitrogen oxides (NO_x) in a lean exhaust gases has become one of the most important environmental concerns. Among the different active phases studied for NO_x reduction reaction, silver-based catalysts supported over alumina show good performances using, as reducing agents, either hydrocarbons or oxygenated compounds. Nevertheless, a good understanding of the mechanism reaction has not been reached yet. This comprehension requires a better characterisation of the silver-based catalysts system. In our study, Ag/Al_2O_3 catalysts showed high efficiency in NO_x reduction using ethanol as reducing agent. The conversion plots, in steady state conditions for the different samples Ag/Al_2O_3 (0.8–3.5% Ag wt), show a great dependance of the activity with the metal loading. The optimal silver loading has been established around 2 wt.% Increasing the silver loading, the temperature of maximal NO_x conversion shifted toward the lower temperatures. According to the literature, a reduced and an oxide phase of silver have been observed by UV–Vis spectroscopy. The ratio between the two phases is changing with the silver loading. However, temperature programmed reduction (TPR) measurements reveal the presence of two types of oxide phases. TPR reveal the coexistence of a silver oxide phase (Ag_2O), according to a production of water in the course of the reaction, and a non-oxygenated phase attributed to isolated Ag^+ cation. Thus, an original way using TPR measurements has been developed to differentiate the various oxidized phases. The aim of this characterisation is to correlate the catalyst's activity with the observed silver phases, in order to understand the nature of phase active for NO_x reduction at low temperatures.

Keywords Silver species · TPR · deNO_x · Ethanol

A. Musi · P. Massiani · D. Brouri · P. Da Costa (✉)
Laboratoire de Réactivité de Surface, CNRS UMR 7609, UPMC, Paris 6, case 178, 4 place Jussieu, 75252 Paris, France
e-mail: patrick.da_costa@upmc.fr

A. Musi · J.-M. Trichard
Renault SA, Technocentre Renault, 1 Avenue du Golf, 78280 Guyancourt, France

1 Introduction

Combustion of hydrocarbons (HC), as source of energy, causes environmental pollution. Theoretically, the products of this combustion are carbon dioxide and water. Nevertheless, the non-ideality of this reaction in the combustion chamber leads to the formation of a large number of pollutants. Among them, nitrogen oxides (NO_x) are not only harmful for human beings but also contribute to environmental pollution by formation of acid rains, thus increasing the green-house effect and participating in the formation of photochemical smog. Current catalytic systems do not allow effective NO_x reduction in conditions of excess oxygen, since modern three way catalysts (TWC) do not work with lean burn mobile engines. Among the different active phases studied for NO_x reduction, alumina supported silver-based catalysts have shown good results using either hydrocarbons or oxygenated compounds as reducing agents [1]. Since precursory work of Miyadera and Koshida [2] on this catalytic system, many studies dealing with the characterisation of silver particles have been performed [3–15]. It is generally believed that cationic silver is predominant for low loaded catalysts, whereas metallic particles prevail when the silver loading is important [11, 12]. Furthermore, oxidized silver state can refer to different silver species, while different oxidized silver species such as isolated Ag^+ cations [3, 6–8, 13, 14], Ag_m^{n+} clusters [3, 7, 8, 13, 14],

and silver aluminate $AgAlO_2$ [7] have been observed. However, any agreement on the nature of the silver active species active for the reaction of NO_x reduction has not been achieved yet. The aim of this article is to reach a better description of the silver particles with a special focus on their oxidation state, morphology, and reactivity using ethanol as reducing agent.

2 Experimental

2.1 Catalyst Synthesis

The γ-Al_2O_3 support was obtained by calcination at 500 °C under air flow during 2 h of a boehmite AlO(OH) provided by Sasol. The catalysts were prepared by excess solvent impregnation of this γ-Al_2O_3 with an $AgNO_3$ aqueous solution. This suspension was stirred and heated under low vacuum conditions in order to evaporate water in mild conditions. After 2 h of maturation at room temperature, the solid was dried overnight at 120 °C. Before the catalytic tests, the catalysts were also calcined in situ under air flow at 500 °C for 2 h. Several Ag/Al_2O_3 samples were prepared depositing loadings of silver ranging from 0.8 to 3.5 wt%, corresponding to different silver loadings, in order to establish optimal silver loading for NO_x reduction and an eventual relation between silver loading and the nature of silver particles. Textural data of the different samples are given in Table 1. Samples are denoted according to their silver loading.

2.2 Methods of Characterisation

The catalyst was characterised by X-ray diffraction (XRD), X-ray photoelectron spectroscopy (XPS), temperature programmed reduction (TPR) measurements, UV–Vis spectroscopy, and transmission electron microscopy (TEM).

The specific surface area (S_{BET}) was also measured using a home made apparatus. Elemental analysis was performed by the "Service Central d'Analyses du CNRS" in order to determine the silver content.

Powder by X-ray diffraction (XRD) was carried out on a Siemens model D-500 diffractometer with CuKα radiation.

Table 1 Textural data of Al_2O_3 support (0Ag) and different Ag/Al_2O_3 samples (*x*Ag)

Sample name	Silver loading (wt%)	BET surface ($m^2\ g^{-1}$)
0Ag	0	220
1Ag	0.8	222
1.5Ag	1.8	213
2.5Ag	2.6	212
3.5Ag	3.5	214

X-ray photoelectron spectroscopy (XPS) spectra were obtained at $P = 10^{-10}$ mbar on a SPECS PHOIBOS 100 spectrometer equipped with a MgKα X-ray source ($hv = 1253.6$ eV). The binding energy values were calibrated against the C 1s peak at 20 eV. Survey spectra were recorded with a 20 eV pass energy and a 150 W electron beam power. High resolution spectra were obtained by applying a window pass energy of 10 eV at 90 °C take off angle (angle between the surface and the analyzer axis). The spectra were curve-fitted using the CASA XPS software and applying a symmetrical Gaussian–Laurentzian (50/50) function.

TPR measurements were performed on an Autochem 2910 Micromeritics apparatus under 5% H_2/Ar flow. The temperature was raised from room temperature to 900° with a heating temperature rate of 10 °C min^{-1}. All TPR measurements were preceded by a temperature programmed oxidation (TPO) under 10% O_2/He to 500 °C with the same temperature heating rate as for TPR. A H_2O-trap was added on the gas line after the reactor. H_2O-trap plunges in a deware containing isopropanol cooled down to −80 °C by mixing it with liquid nitrogen. The purpose of this trap is to condense the water produced during the reduction reaction. Water has an influence upon the signal of the detector and its presence does not allow a correct integration of the reduction peaks for the quantification of the H_2 consumption.

Diffuse reflectance UV–Vis spectra were recorded at room temperature between 190 and 2500 nm on a Varian Cary 5E spectrometer equipped with a double monochromator and an integrating sphere coated with polytetrafluoroethylene (PTFE). PTFE was the reference.

High resolution transmission electron microscopy (HRTEM) was performed to identify the location and the size of the silver particles on alumina and to check their dispersion. The HRTEM studies were performed on a JEOL-JEM 2011 HR (LaB) microscope operating at 200 kV.

2.3 Catalytic Measurements

Temperature-programmed surface reaction (TPSR) and steady state experiments were carried out, in a U-type glass reactor, using gas mixture consisting of 500 ppm NO + 2,500 ppm C_1 C_2H_5OH + 10% O_2 in Ar. The gases (NO, O_2, and Ar) were fed from compressed cylinders provided by Air Liquide and adjusted with Brooks mass flow controllers (5850 TR). Ethanol was supplied to the reacting stream by means of two temperature-controlled bubble towers (purged by Ar flow): a saturator at room temperature and a condenser at −5 °C. The total flow rate of the feed gas was maintained at 250 mL min^{-1} for all experiments. The gas hour space velocity (GHSV) was equal to 40,000 h^{-1}. The sample (320 mg) was held on plugs of quartz wool and the

temperature was controlled through a WEST 4000 temperature controller using a K-type thermocouple. The composition of the reactor outflow was continuously measured using a set of specific detectors. An Eco Physics CLD 700 AL chemiluminescence NO_x analyser (for NO and total NO_x (i.e., NO + NO_2)) allowed the simultaneous detection of NO and NO_x. Two Ultramat 6 IR analysers were used to monitor N_2O, CO, and CO_2. A FID detector (Fidamat 5) was used to follow the concentration of the hydrocarbonated compounds.

3 Results and Discussion

3.1 Morphological and Structural Characterisation

Impregnation method we used does not modify in a significant manner high specific surface of the support (Table 1). The XRD patterns of all samples, after calcination and even after reaction up to 500 °C, showed identical aspect dominated by the γ-Al_2O_3 component. No peaks attributable to Ag^0, Ag_2O, or $AlAgO_2$ phases were observed. This fact suggests a good dispersion of the silver particles upon the support.

Analysis of TEM images could not reveal the presence of any Ag-containing particles for freshly calcined samples. Since the presence of silver has been shown by EDS, this lack of visibility confirms the good dispersion of silver upon the support. However, numerous silver particles, with a diameter below 5 nm, are detected after TPSR as is seen for the 2.5Ag sample taken as a representative example (Fig. 1). This fact suggests that a sintering of the silver species takes place under reaction conditions. The particles intereticular distance was measured (2.4 Å) and it seems to correspond to the (111) plane of metallic silver (JCPDS 03-065-2871).

3.2 Nature of the Silver Species

The UV–Vis spectra of the calcined samples are showed in Fig. 2a. Major peaks at 212, 260, 290, 330, and 437 nm are observed. The peaks at 212 and 260 nm are generally attributed to the $4d^{10}$ to $4d^9s^1$ transition of highly dispersed Ag^+ cations [3, 7, 10]. Due to the strong absorption of Al_2O_3 at these wavelengths the attribution could be inaccurate. However, since the peak at 260 nm varies in intensity and position when the silver loading increases, a possible attribution of this peak to Ag^+ isolated cations is advanced. The peak at 290 nm, not observed for the 1Ag sample, could not be attributed with accuracy. In the literature, it has been assigned, together with a peak at 350 nm, to Ag_n^{m+} clusters [7]. Also it was proposed that

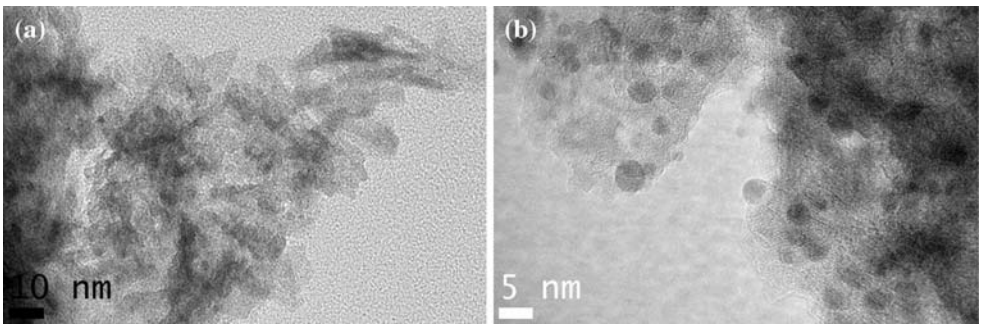

Fig. 1 TEM of the 2.5Ag sample **a** freshly calcined and **b** after SCR reaction

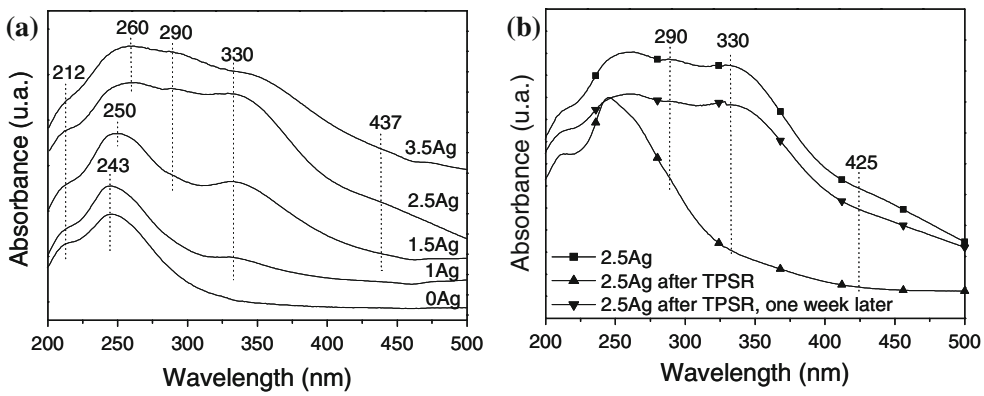

Fig. 2 Diffuse reflectance UV–Vis spectra of **a** support and Ag/Al_2O_3 fresh samples and **b** Ag/Al_2O_3 after TPSR with ethanol as reductant

this peak is due to electronic transitions of reduced Ag species [14]. Finally, it could also correspond to the shifted peak of silver aluminate, normally observed at 230 nm [7]. The attribution of the peak at 330 nm is clearer, this peak being indicative of the presence of Ag_n^{m+} clusters [3, 7, 8, 13, 14], while the peak at 437 nm is assigned to metallic silver particles [3, 7, 10, 14]. After the freshly calcined samples, catalysts exposed to reaction conditions were also analysed.

In Fig. 3b spectra of the 2.5Ag sample after TPSR experience is shown. Comparing it with a freshly calcined sample, it is noticed that all the peaks situated at wavelengths higher than 275 nm drastically decrease in intensity. The concerned peaks are these unambiguously attributable to Ag_n^{m+} clusters and to metallic particles. Moreover, the colour of the sample is frankly modified, changing from yellow ocher into white after TPSR. During 1 week, the sample obtained after TPSR was exposed to light and air. It was noticed that after such a period the sample recovered its initial colour and an UV–Vis spectra was very similar to the one corresponding to the fresh catalyst. This light instability when the catalyst is exposed to light is assigned to the formation of silver nitrate under reaction conditions [16]. Silver nitrate formation has already been observed in the literature [15] when a similar Ag/Al_2O_3 catalyst was exposed to O_2/NO flow. These observations seem to indicate that the exposition of catalyst to reaction conditions modifies drastically the nature of the silver species observed in samples freshly calcined.

3.3 Oxidation State of Silver Particles

XPS runs have been performed in order to determine the reduction degree of each sample. The XPS spectrum of the 2.5Ag sample freshly calcined is presented in Fig. 3. Deconvolution of the $3d_{5/2}$ peak shows the presence of two contributions at 367.5 and 368.5 eV, which are attributed, according with literature [6], to Ag_2O and Ag^0, respectively. The quantitative analysis of the spectrum has been performed in order to establish the content of metallic phase. Results are presented in Table 2. The silver loading has no influence upon the reduction degree of the analysed samples. The metallic silver content is approximatively of 70% for each sample.

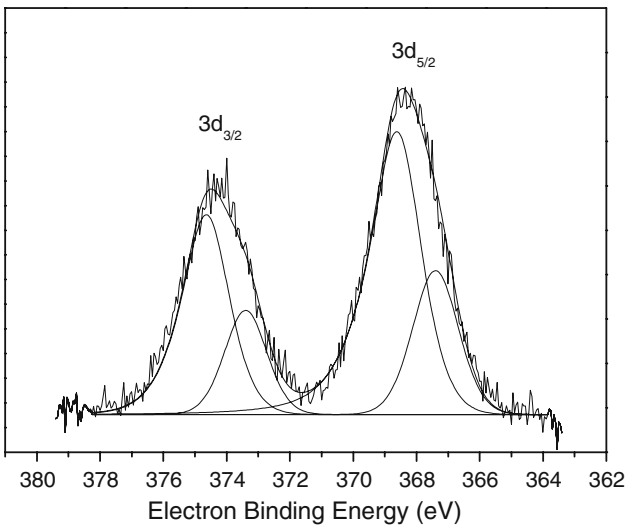

Fig. 3 XPS Ag(3d) spectra of 2.5Ag sample

H_2-TPR measurements were performed in order to study the reducibility of silver species (without H_2O-trap) and to quantify (with H_2O-trap) the metallic silver content so to confirm the results obtained by XPS spectroscopy. The TPR profiles, presented in Fig. 4, were obtained without the H_2O-Trap, so the water production influences the signal. Since a TPO is performed in situ systematically before each TPR experience, no water corresponding to hydration phenomenon is present. The negative peak observed at high temperature is attributed to water production by alumina dehydroxylation. The most important hydrogen consumption, observed at 275 °C for 3.5Ag sample, is shifted towards higher temperatures with decreasing silver loading. This main H_2-consumption peak is attributed to the reduction Ag_2O clusters [5, 8, 14]. It is supposed that Ag_n^{m+} clusters detected by UV–Vis spectroscopy correspond to the Ag_2O oxidised phase. The support does not present any H_2 consumption peaks in the temperatures range when the reduction of the silver oxidised phase is observed. Furthermore, a shoulder is observed at 140 °C. Since the UV–Vis characterisation revealed the presence of Ag^+ cations, it is supposed that this shoulder is due to Ag^+ cations reduction.

To confirm this assumption a method to differentiate between Ag^+ cations and Ag_2O nanoparticles was developed. The basic difference between these two silver phases is that the reduction of Ag_2O produces water, whereas isolated Ag^+ cations does not. An approach based on this distinction has been implemented to distinguish the two oxidised phases. Thus the H_2-TPR experiments were performed using an H_2O-trap. Firstly, the temperature was raised to 150 °C and holded in order to reduce the Ag^+ cations. During the temperature plateau, the H_2O-trap was

Table 2 Metallic silver content determined by XPS analysis and TPR measurements

Sample	Metallic silver content by XPS (%)	Metallic silver content by TPR (%)
1Ag	69	72
1.5Ag	67	67
2.5Ag	72	74
3.5Ag	73	70

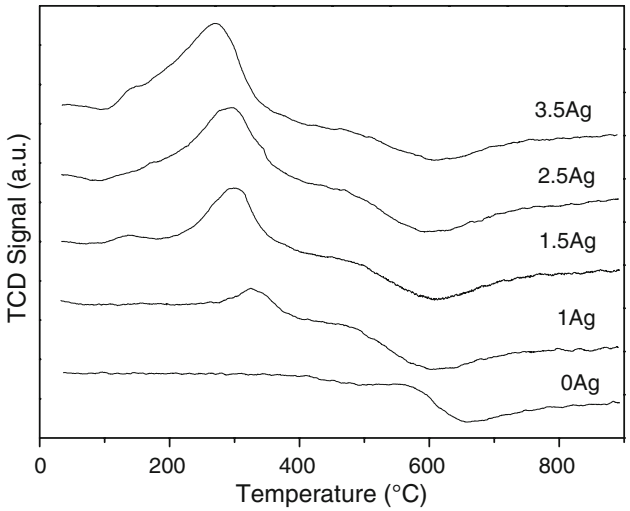

Fig. 4 TPR profiles, normalized to catalyst mass, of support and Ag/Al_2O_3 fresh samples

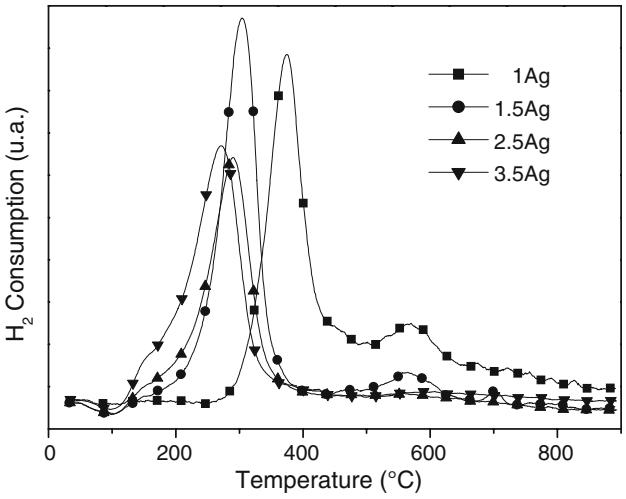

Fig. 6 TPR profiles, normalized to silver content, of Ag/Al_2O_3 fresh samples using H_2O-trap

removed so that eventually trapped water could desorb and be detected. Then, the H_2O-trap was placed and the same proceeding was repeated at 350 °C so in order to reduce Ag_2O phase. According to our hypothesis, the reduction peak at 150 °C does not produce any water desorption, whereas the peak at 350 °C is followed by a water desorption (negative peak) when H_2O-trap is removed (Fig. 5).

By comparing the intensity of the peaks obtained at 150 °C, the presence of Ag^+ seems to be favored for higher silver loadings. Finally, we repeated the standard H_2-TPR measurements including the H_2O-trap (Fig. 6). Integrating the areas of the peaks the amount of oxidized silver content for each sample was obtained. The results are in agreement with the values obtained above by XPS spectroscopy and confirm a reduction degree of about 70% for each sample

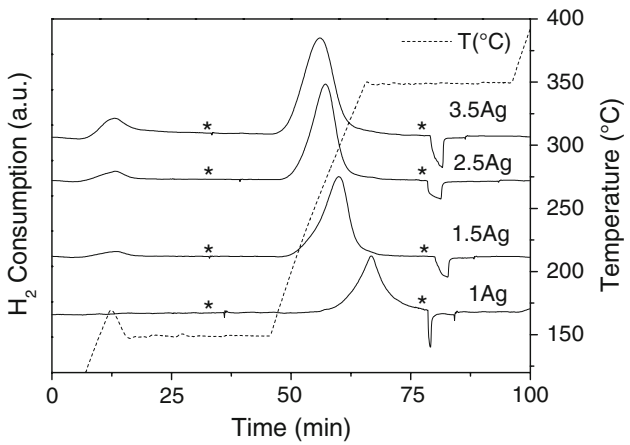

Fig. 5 TPR profiles, by temperature stages, of Ag/Al_2O_3 fresh samples using a removable H_2O-trap (* indicates the moment when the H_2O-trap is removed)

(Table 2). The appearance of a TPR peak at 570 °C could be due to silver aluminate although this attribution needs further investigation.

3.4 Catalytic Activity: Effect of Silver Loading

The NO_x and ethanol conversions, obtained for each sample and shown in Fig. 7, indicate that temperature of maximum NO_x conversion decreases with increasing silver loading. Simultaneously, it was observed the same phenomenon for light-off temperature of ethanol oxidation reaction. The highest NO_x conversion rate is obtained with the 1Ag sample. According to the literature [9, 13], optimal silver loading for NO_x reduction is around 2 wt%. In agreement, the 2.5Ag sample provides better activity at lower temperatures but avoiding an important loss of conversion at higher temperatures like with 3.5Ag sample. For the 2.5Ag sample N_2 yields measurement were performed. For this sample selectivity to N_2 is included in the range from 60% at 300 °C to 80% at 475 °C. Since silver metallic and oxidized phases are present in equal content in all samples, it is not clear which phase improves catalyst activity at lower temperatures when silver charge is increased. It is known that metallic silver particles enhance reductant oxidation [17]. It is seen (Fig. 7b) that ethanol is oxidised at lower temperatures with increasing of silver content. It can be assumed that this phenomenon is due to a higher metallic silver content according with a more important silver charge. Since temperature of maximum NO_x conversion follows the same behaviour, it can be proposed that metallic silver particles also ameliorate NO_x reduction at lower temperatures. However, it has been evidenced that Ag^+ isolated cations content increases with silver loading (Figs. 4 and 5). Thus, it can be also

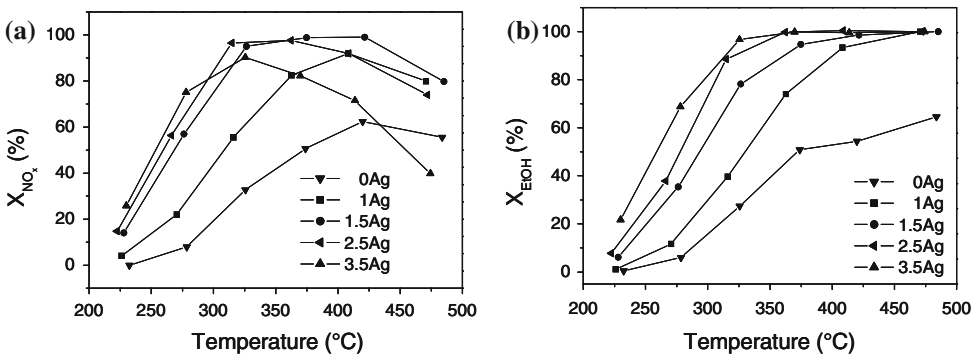

Fig. 7 Effect of silver loading over γ-Al_2O_3 for C_2H_5OH-SCR of NO_x. **a** NO_x conversion; **b** ethanol conversion

speculatively advanced that this species promotes catalyst's activity at lower temperatures.

4 Conclusion

Coexistence of an oxidised and a metallic phase is typical for silver based alumina supported catalytic system. According to the literature, the presence of different silver particles, Ag^+ isolated cations, Ag_n^{m+} clusters and Ag^0, has been evidenced for freshly calcined samples. No silver aluminate has been detected. Oppositely the general belief, the metal loading has no influence on silver species nature. For every synthesised sample, corresponding to different silver loadings, XPS spectroscopy and H_2-TPR (performed with H_2O-trap) revealed the same ratio between the metallic and the oxidised silver phases. An original H_2-TPR methodology, based on water production detection, has been developed to distinguish between Ag^+ and Ag_2O among the oxidised phase. The content of isolated Ag^+ cations seems to increase with silver loading. However, nature of silver species is drastically modified when the catalyst is exposed to C_2H_5OH-SCR reaction conditions. Then, the formation of $AgNO_3$ is strongly promoted. Finally, a correlation between silver particles nature and catalyst's activity has been advanced, although strictly conjectural.

References

1. Kameoka S, Ukisu Y, Miyadera T (2000) Phys Chem Chem Phys 2:367
2. Miyadera T., Koshida K., Chem Lett (1993) 1483
3. Keshavaraja A, She X, Flytzani-Stephanopoulos M (2000) Appl Catal B 27:L1
4. Martinez-Arias A, Fernandez-Garcia M, Iglesias-Juez A, Andreson JA, Conesa JC, Soria J (2000) Appl Catal B 28:29
5. Kung MC, Kung H (2000) Top Catal 10:21
6. Richter M, Langpape M, Kolf S, Grubert G, Eckelt R, Radnik J, Schneider M, Pohl M-M, Fricke R (2002) Appl Catal B 36:261
7. Bogdanchikova N, Meunier FC, Avalos-Borja M, Breen JP, Pestryakov A (2002) Appl Catal B 26:287
8. Richter M, Bentrup U, Eckelt R, Schneider M, Pohl M-M, Fricke R (2004) Appl Catal B 51:261
9. Brosius R, Arve K, Groothaert MH, Martens JA (2005) J Catal 231:344
10. She X, Flytzani-Stephanopoulos M (2006) J Catal 237:79
11. Meunier FC, Ukropec R, Stapleton C, Ross JRH (2001) Appl Catal B 30:163
12. Burch R, Breen JP, Meunier FC (2002) Appl Catal B 39:283
13. Shimizu K-I, Shibata J, Yoshida H, Satsuma A, Hattori T (2001) Appl Catal B 30:151
14. Son IH, Kim MC, Koh HL, Kim KL (2001) Catal Lett 75:191
15. Brosius R, Arve K, Groothaert MH, Martens JA (2005) J Catal 231:344
16. Parkes GD (1961) Mellor's modern inorganic chemistry. Longmans, London
17. Meunier FC, Breen JP, Zuzaniuk V, Olsson M, Ross JRH (1999) J Catal 187:493